Tip-jump statistics of stick-slip friction

A. Schirmeisen, L. Jansen, and H. Fuchs
Center for Nanotechnology (CeNTech) and Physikalisches Institut, Westfälische Wilhelms-Universität Münster, Wilhelm-Klemm-Strasse 10, 48149 Münster, Germany
(Received 27 August 2004; published 3 June 2005)

Friction maps with atomic unit cell periodicity on highly oriented graphite in ultra-high vacuum are measured with the friction force microscope. The well-known stick-slip phenomenon is observed where the tip jumps between individual equilibrium positions. We perform a statistical analysis of the frictional forces that are necessary to induce the tip jumps. The corresponding histograms give a direct fingerprint of the distribution function of the tip-jump events. The histograms depend strongly on the atomic structure of the surface, which is related to the two-dimensionality of the surface potential. We compare the experimental to the theoretical distribution function, which is based on the thermally activated Tomlinson model for atomic friction, and quantitative values for the effective energy barriers are extracted.

DOI: 10.1103/PhysRevB.71.245403 PACS number(s): 68.37.Ps, 46.55.+d, 07.79.Sp, 81.40.Pq

I. INTRODUCTION

The understanding of friction properties at the nanoscale remains a challenge to scientists and engineers in a wide range of disciplines. One of the fundamental processes of sliding friction is the "stick-slip" phenomenon. Already many decades ago, Tomlinson[1] and Prandtl[2] developed a theory which tried to establish a correlation between macroscopic friction and microscopic stick-slip processes. With the invention of the atomic force microscope (AFM)[3] it became possible to observe sliding friction processes with atomic periodicity,[4] opening up the possibility for a direct investigation of atomic scale friction. The surface of highly oriented graphite (HOPG) has been the focus of several experimental studies with the AFM,[5,6] due to its relative inertness and technological relevance as an efficient lubrication material. Atomic scale friction maps on HOPG have been interpreted in terms of a two-dimensional hopping motion of the tip between different equilibrium positions.[7–9]

If the temperature is nonzero, the hopping or jump process is of statistical nature. Gnecco *et al.*[10] were the first to apply this idea to stick-slip friction measurements. As a direct consequence they found that stick-slip friction depends logarithmically on the tip sliding velocity. Sang *et al.*[11] have investigated theoretically these jump processes and presented an analytical expression for the corresponding statistical distribution function.

In this paper we focus on the statistics of these jump processes. We extract the probability distribution of the jumps from experimental friction force maps on HOPG. The results are compared to the statistical distribution function from Sang *et al.*[11] Quantitative values for the parameters that govern the friction process can be extracted from the fit to the model.

The paper is structured as follows: First, we will review the thermally activated Tomlinson model after Sang *et al.*[11] In the experimental part the stick-slip experiments are presented followed by the method, which allows us to extract the distribution function of the tip jumps from the experimental friction maps. Finally, the experimental and theoretical distribution functions are compared.

II. THEORETICAL BACKGROUND

The Tomlinson model[1] has been successfully used to explain the stick-slip phenomenon with atomic peridocity. In this model it is assumed that a pointlike tip at position x_t, which is coupled elastically to the microscope body at position x_M, is moving in a periodic tip-sample interaction potential $V(x)$. Assuming a sinusoidal interaction potential $V(x) = E_0 \cos(2\pi x/a)$, with a surface barrier potential height[12] E_0 and a lattice constant a, the corresponding equation of motion is

$$m^* \ddot{x}_t = c_{eff}(x_M - x_t) - \frac{2\pi E_0}{a} \sin\left(\frac{2\pi x_t}{a}\right) - m^* \gamma \dot{x}_t. \qquad (1)$$

Here c_{eff} is the effective lateral spring constant describing the elastic coupling of the tip with the microscope base, which includes the elastic behavior of the cantilever and the tip-sample contact.[13] The factor γ is the microscopic friction coefficient, which was introduced by Hölscher *et al.*[7] to describe the loss of energy during the slip movement as a velocity-dependent process. Solving this equation leads to a solution describing the stick-slip movement of the tip at zero temperature.

For better clarity, the corresponding potential diagram is shown in Fig. 1. The tip is trapped in a local potential minimum. An energy barrier of height ΔE prevents the tip from reaching the next energy minimum to the right. The tip base moves with velocity v, and at a certain position $x_M = x_{M,jump}$ the local minimum vanishes and the tip "jumps" to the next local minimum. The jump height, i.e., the maximum force just before the slip-event occurs, is a direct function of the surface barrier potential E_0, the effective mass m^*, the effective spring constant c_{eff}, and the lattice constant a.

At nonzero temperatures, however, the jump event becomes a statistical process. In previous publications Gnecco *et al.*[10] and Sang *et al.*[11] have taken the influence of a finite tip-sample temperature into acount and found as a result that the temperature will induce a velocity dependence of the friction, which was verified experimentally.[10] Additionally, an analytical description for the theoretical probability distri-

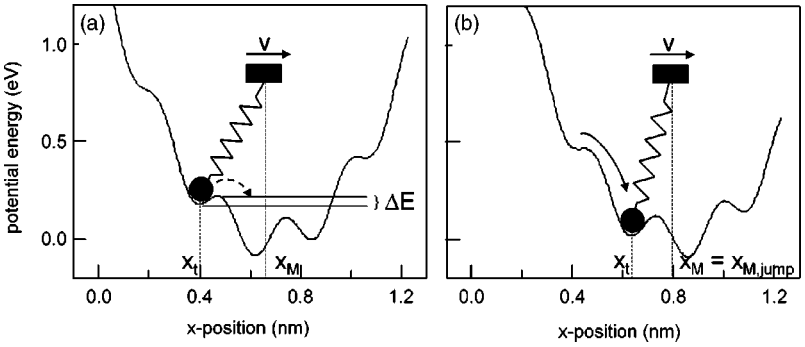

FIG. 1. The potential diagram of the Tomlinson model at zero temperature. In (a) the tip is trapped in a local minimum and is separated from the next minimum to the right by an energy barrier of height ΔE. In (b) the tip base has moved to the right, and the energy barrier has vanished, which causes the tip to "jump" to the next local minimum. However, at nonzero temperature, there is a finite probability that the tip jumps over the energy barrier already in (a) (dashed arrow).

bution function of the individual jumps was derived.[11] However, a statistical analysis of experimental stick-slip events has not been presented so far.

The analytical formula for the jump probability from Sang *et al.*[11] can be written as a function of the so-called reduced bias f^*:

$$P(f^*) = \frac{3}{2}\frac{f^{*1/2}}{v^*}\exp(-f^{*3/2} - e^{f^{*3/2}}/v^*). \tag{2}$$

The dimensionless velocity v^* is defined according to[11]

$$v^* = \frac{v\gamma c_{eff} a}{2\pi^2 k_B T f_{tc}^2}\cdot\frac{\Omega_k^2}{\sqrt{1-\Omega_k^4}} \tag{3}$$

with $\Omega_k = \sqrt{c_{eff}a^2/4\pi^2 E_0}$, which is the ratio of the resonance frequency of the tip in the surface potential E_0 versus the torsional resonance frequency of the tip in contact f_{tc}. The reduced bias f^* is a direct function of the lateral force F_m, at which a jump is induced:

$$f^* = \left(\frac{2E_0}{3k_B T}\right)^{2/3}\frac{\Omega_k^2}{(1-\Omega_k^4)^{1/6}}\frac{4\pi}{c_{eff}a}(c_{eff}R_c - F_m). \tag{4}$$

The critical position R_c, where the effective barrier height vanishes, is defined as $2\pi R_c/a = \arccos(-\Omega_k^2) + \Omega_k^{-2}\cdot\sin[\arccos(-\Omega_k^2)]$. Combining Eqs. (2)–(4) yields the analytical description of the jump probability as a function of the jump-heights F_m. An example for the normalized distribution function is shown in Fig. 2. Typical parameters taken from our experiments were chosen: temperature $T=300$ K, lattice constant of HOPG $a=0.246$ nm, tip scan velocity of $v=80$ nm/s, effective spring constant $c_{eff}=1$ N/m, friction coefficient $\gamma=1\times10^6$ s^{-1}, and resonance frequency $f_{tc}=75$ kHz. The energy barrier height E_0 was varied between 100 and 160 meV, resulting in four different histograms. The histograms can be characterized by four parameters: the width of the peak, the height of the peak, the asymmetry of the peak, and the position of the peak with respect to the force axis. The difference in the energy barrier causes a large change of the lateral position of the peak by a factor of 2.3, while the height and width only change by 16% in the considered regime. For increasing energy barriers the lateral force needed to jump over the effective barrier height is higher, inducing a shift of the peak to larger values. However, the width of the distribution is mainly caused by the temperature, which causes the jump process to become of statistical nature. For example, at zero temperature the distribution function would become a delta peak.

III. FRICTION EXPERIMENTS

The friction force experiments were conducted in a commercial atomic force microscope (AFM) under ultra-high vacuum (UHV) conditions at room temperature (Omicron VT-AFM). The sample was highly oriented pyrolytic graphite (HOPG) that was cleaved in the load lock in vacuum at $p=1\times10^{-9}$ mbar shortly before the AFM experiments. As force sensors we used single crystalline, rectangular silicon cantilevers (LFMR-type from Nanosensors) with a width of $W=42$ μm, a length of $L=214$ μm, and a tip height of $H=15$ μm (data supplied by manufacturer). The thickness of the cantilevers was determined from the resonance frequency of the normal oscillation f_n measured in vacuum.[14] The normal (c_n) and torsional (c_t) spring constants of the cantilever

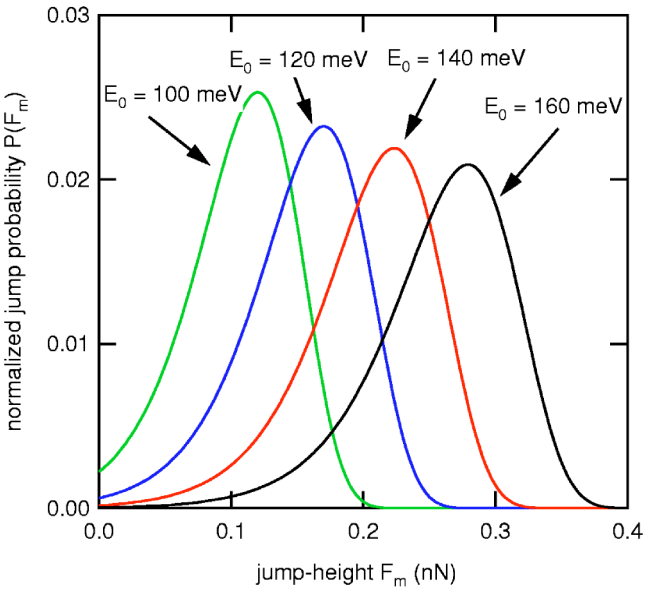

FIG. 2. (Color online) The relative probability that a jump occurs as a function of the maximum lateral force F_m, which was necessary to induce the jump, after the analytical derivation of the thermally activated Tomlinson model from Sang *et al.* (Ref. 11). Typical parameters encountered during the experiments were chosen (see text). The four histograms represent the cases for different energy barrier heights E_0.

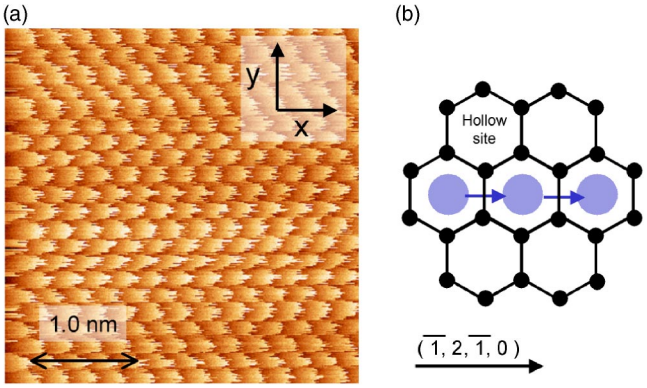

FIG. 3. (Color online) (a) A 3×3 nm^2 lateral friction force map on HOPG at tip base scan velocity $v=60$ nm/s. (b) The schematic representation of the HOPG unit cell. The solid black circles are the carbon atoms in the top layer which are arranged hexagonally around a hollow-site. The big blue circles represent the equilibrium positions where the tip would stick and the blue arrows indicate the jump or slip process.

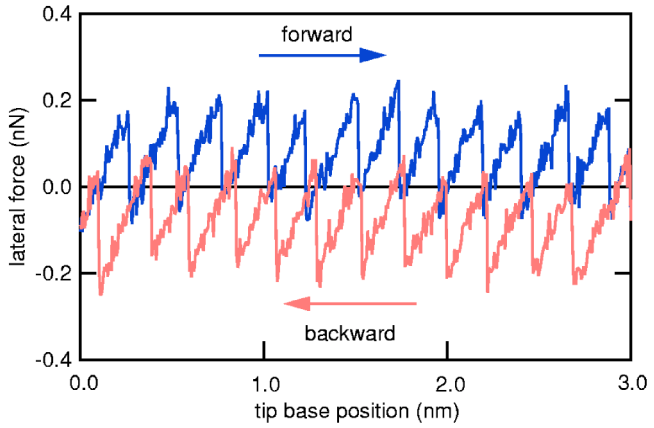

FIG. 4. (Color online) The friction loops from the friction map in Fig. 3(a) showing the stick-slip behavior of the scanning tip in the trace (blue) and retrace (red) directions at a tip base velocity of 60 nm s^{-1}.

were calculated from the geometric dimensions[15] yielding $c_n=0.12$ N m^{-1} and $c_t=14.0$ N m^{-1} (with the E-modulus $E=169$ GPa and shear modulus $G=50$ GPa, data supplied by the manufacturer).

For quantitative interpretation of the normal and frictional forces we calibrated the sensitivity of the AFM. Once the tip was in contact, we performed force distance curves, where we assumed that the contact is much stiffer than the cantilever spring constant. From the slope of the force distance curves we determined the sensitivity of the normal direction. For the calibration of the torsional twisting of the cantilever induced by the frictional forces we used the method from Bilas *et al.*[16] This method is only applicable to systems with a beam deflection detection system and only in the case that the tip is scanned and the sample is fixed. The method relies on the effect that a bending of the piezotube during scanning induces a small angle between the cantilever and the incident laser beam.

The adhesion force between the tip and the sample during the following friction force experiments was determined from the average jump-off-contact value ($F_{off}=11.0$ nN) of several force-distance curves. No additional load was applied in order to prevent any further changes in the atomic configuration of the tip-sample contact. Hence, the effective load during the friction experiments is entirely determined by F_{off}.

After the tip was approached towards the surface, a large area (1×1 μm^2) of the HOPG sample was scanned in order to verify that a flat and homogeneous part of the surface with no steps was investigated. Then small areas of the sample were scanned while the tip-sample distance feedback loop was switched off. Each line is scanned in the forward and backward direction of the fast scan direction. A typical 3×3 nm^2 friction force map, i.e., the friction force as a function of tip base position, is shown in Fig. 3(a). The well-known stick-slip phenomenon is observed which leads to the friction force contrast with atomic unit cell periodicity of the surface. The friction signal for a single scan line in the forward (blue) and backward (red) directions is shown in Fig. 4 and shows a sawtooth type behavior. The stick part is characterized by a linearly increasing or decreasing F_L signal as a function of the lateral tip base position. In this case, the tip sticks at the position between the surface atoms and while the tip base moves continuously the cantilever is twisted. If the lateral force due to the twisting is large enough, the tip will jump laterally to the next equilibrium position, causing the sudden vertical change in F_L. The area embraced by the two friction scan lines represents the energy that was dissipated during this friction loop.

The individual carbon atoms form hexagonal rings that are arranged in a honeycomb structure[7] [see also Fig. 3(b)]. During the scan the tip will jump in between the local energy minima, which are located at the center of the carbon rings, the so-called "hollow sites" of the HOPG surface[7] [blue circles in Fig. 3(b)]. In general these jumps will follow a two-dimensional zig-zag path on the surface,[8,9] leading to a movement of the tip along the fast scan direction as well as perpendicular to it. Due to this effect, contrast will not only appear in the lateral force signal F_L, but also in the normal force signal F_N, which complicates the analysis of single jumps considerably. In order to minimize this effect we oriented the sample in such a way that the fast scan direction (x direction) scans along the $(\bar{1},2,\bar{1},0)$ direction of the (0001) HOPG surface. In this case, the tip will perform almost exclusively jumps along the rows of the hollow-sites as indicated by the blue arrows in Fig. 3(b). Only if the the next row along the y direction is reached will the tip perform one jump perpendicular to the scan direction.

IV. STATISTICAL ANALYSIS OF INDIVIDUAL JUMP HEIGHTS

In the following we investigate the statistical distribution of single tip jumps during the friction loops. A good experimental observable is the maximum lateral force F_m during the stick part just before the individual jumps, i.e., slip-events, occur. For simplicity in the further discussion we call

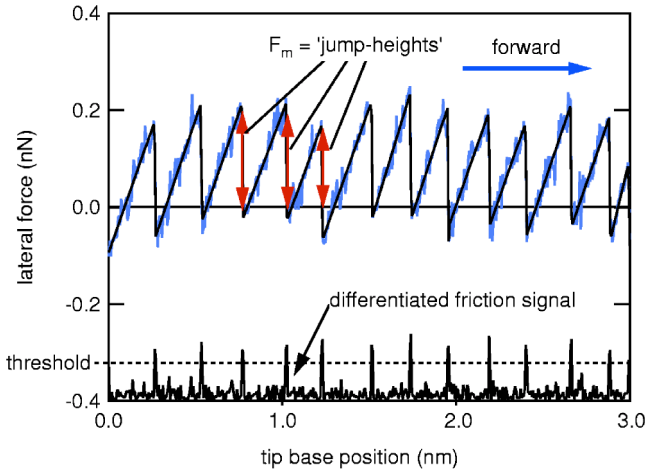

FIG. 5. (Color online) The jump height analysis: The raw data of a single friction trace (blue line) is shown as a function of the tip base position. The differentiated friction signal (black line, bottom) is used to find the position of the slip events, by comparison with an appropriate threshold value (dotted line). The raw data between the slip positions is fitted with a line (black line) and the maximum of the lateral force just before the slip events is then extracted as the jump-height, i.e., the F_m value (red arrows).

this maximum force F_m the "jump-height." We developed a method to extract the jump-heights with sufficient accuracy from the raw data. First, the average of the forward and backward line scans is calculated and fitted with a straight line that defines the zero friction line. A typical forward friction raw signal corrected by the zero friction line is shown in Fig. 5 (blue line).

Second, in order to find the lateral position of a jump, the raw data signal is numerically differentiated (black line at the bottom of Fig. 5) and the tip base positions where the differentiated signal is above a certain threshhold (dotted line in Fig. 5) are determined. Then each individual stick part of the friction curve is fitted with a line (upper solid black line in Fig. 5). The height of the peaks is then extracted, yielding the individual jump-heights F_m. Please note that the jump-height is always measured with respect to the zero friction line. This procedure takes advantage of all the data points acquired during the friction scan, which allows an improved signal-to-noise ratio for the jump-height determination.

Figure 6 shows a typical "jump-height histogram," i.e., the number of jumps as a function of the maximum lateral force F_m just before the jump. The histograms were compiled from a 6×6 nm^2 friction map at a scan speed $v=120$ nm s^{-1}. A total of 23 748 jumps were extracted from the friction map. The jumps were collected in bins with a width of 0.008 nN, which is a compromise between resolution and smoothness of the resulting histogram. For comparison with the theoretical jump distribution function the histogram must be normalized by the total number of jumps. The right-hand scale shows the corresponding relative jump probability. The overall shape of the curve roughly resembles the theoretical curve for the distribution function in Fig. 2. A quantitative comparison will follow in the next sections.

We intentionally adjusted the sample orientation such that only jumps parallel to the fast scan direction (x direction)

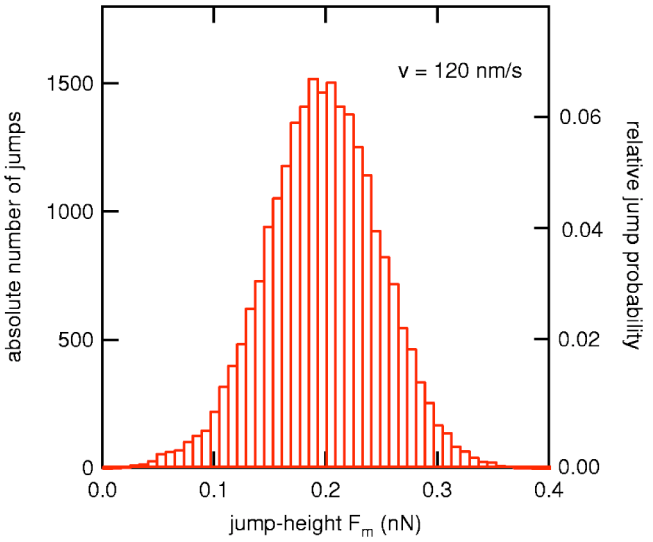

FIG. 6. The experimental jump-height histogram for a tip base velocity of 120 nm s^{-1}. The number of jumps is shown as a function of the lateral force necessary to induce the jump. A total of 23 748 jumps were analyzed for this histogram, and a bin width of 0.008 nN was chosen. The right-hand scale shows the relative jump probability, which is the number of jumps from the left-hand scale divided by the total number of jumps.

occur. Therefore we expected that a one-dimensional model for atomic friction would be a good approximation. However, in Fig. 7 we show a zoom of a typical friction map together with a plot for the dissipated energy per friction loop per atomic unit cell (with $a=0.246$ nm), which is defined as the area between trace and retrace divided by the number of unit cells along the scan line. Clearly, the dissipated energy varies substantially from 10 to 30 eV with the tip position along the slow scan axis (y direction), depending on whether the tip scans exactly along the center of the hollow-site rows (e.g., solid arrows) or between two rows of

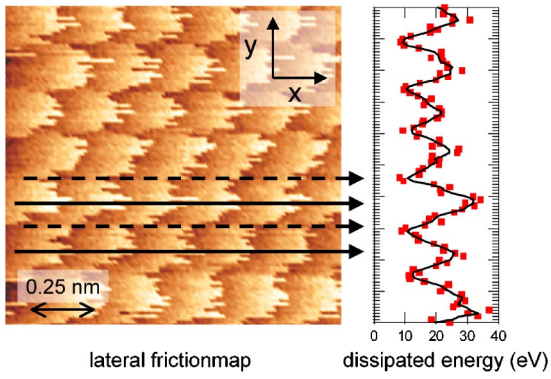

FIG. 7. (Color online) The left image shows a zoom of the friction map of image size 6×6 nm^2 at a scan speed of 60 nm s^{-1}. The dissipated energy was calculated from the individual friction loops and is shown in the right part of the graph. For better comparison with other measurements, the dissipated energy is normalized by the number of lattice unit cells, over which the tip was scanned. The black line is a 3-point box average of the raw data (squares) and is meant as a guide to the eye.

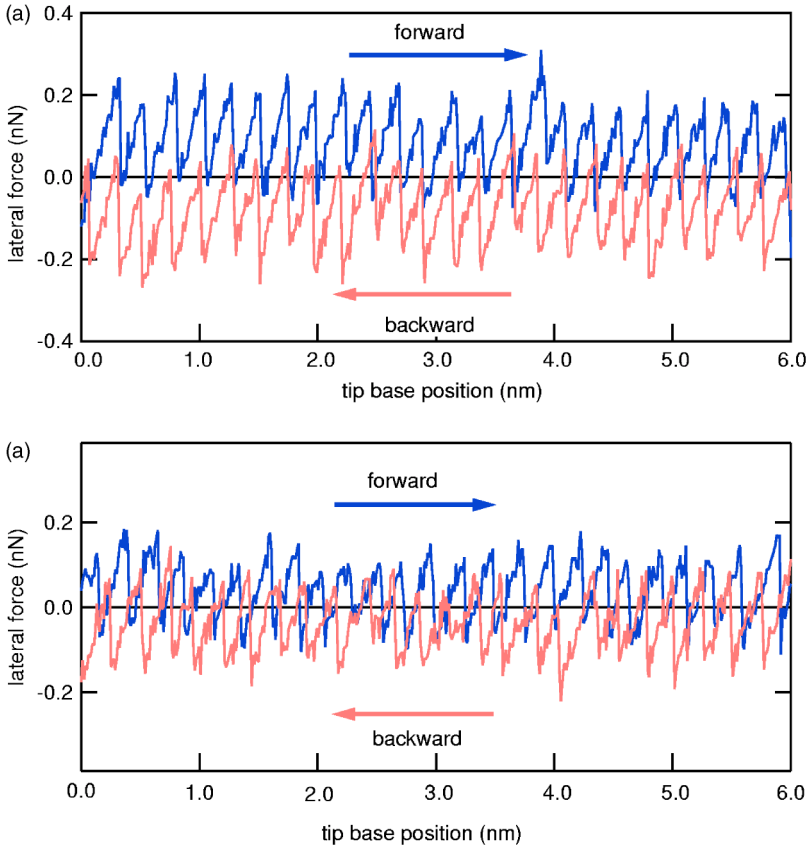

FIG. 8. (Color online) The friction loops extracted from the friction map in Fig. 7(a) showing the stick-slip behavior of the scanning tip in the trace and retrace direction on two different positions of the surface: (a) along the center of the hollow-sites [blue lines in Fig. 7(a) and 7(b)] between two hollow-site rows [red lines in Fig. 7(a)]. The dashed lines show the fitted zero friction line which serves as the reference for the jump-height determination.

hollow-sites (e.g., dashed arrows). The friction loops also look very different depending on the exact position of the tip along the y direction. Figures 8(a) and 8(b) show, for example, typical friction loops along the center of the hollow-site rows and between the rows, respectively. Therefore, some crucial parameters governing the atomic friction process must change considerably, depending on the y position of the tip.

Since the average friction depends strongly on the exact tip position in the y direction, a one-dimensional model must be insufficient to describe the system adequately. It is therefore necessary to separately analyze the situations where the tip is in the center and on the side of the hollow-site rows. So far, the jump-height histogram in Fig. 6 represents an average over different sites. In this context it should be noted that the appearance of the two-dimensional friction maps can change considerably also under different loads.[17]

In Fig. 9 (scan speed $v=80$ nm/s) and Fig. 10 (scan speed $v=120$ nm s^{-1}) we present experimental jump-height distribution functions (solid cityscape lines) that are created from the jumps occuring in the center of the hollow-site rows (solid arrows, compare also Fig. 7) and between the rows (dashed arrows). Each diagram is compiled from about 6000 jumps out of a total of 24 000 jumps, to achieve sufficient statistics. Although a certain averaging over different sites can still not be excluded, these histograms represent now the almost one-dimensional stick-slip case and will be compared to the thermally activated Tomlinson model in the next paragraph.

V. COMPARISON OF EXPERIMENTAL AND THEORETICAL JUMP STATISTICS

In order to compare our experimental jump-height distribution diagrams to the theoretical curves we first analyze the relevant fit parameters of the system. From the experiment the tip-sample temperature $T=300$ K, the HOPG unit cell lattice constant $a=0.246$ nm, and the relative tip-sample velocity v are known. The effective lateral spring constant is derived from the slope of the stick-part of the friction curves[13] yielding $c_{eff}=1.02\pm0.16$ N m^{-1}. The torsional resonance frequency of the tip in contact f_{tc} can be estimated:[18] The free torsional resonance frequency was measured directly in the UHV chamber ($f_{tf}=274\,948$ Hz). Assuming that the effective mass does not change if the tip is in contact with the surface, the resonance frequency scales with $\sqrt{c_{eff}/c_t}$, giving an estimate for $f_{tc}=73\,482$ Hz. For triangular cantilevers, f_{tc} values of comparable magnitude have been reported before.[18]

The only unknown parameters left are the friction coefficient γ, describing the rate at which the kinetic energy of the tip is dissipated, and the surface barrier potential E_0. However, the fit of the theoretical distribution function to the experimental histograms does not allow an independent determination of both parameters. In our case, we will use an estimate for the friction coefficient γ. The ratio of γ versus f_{tc} determines the type of damped oscillation behavior. For theoretical studies of the Tomlinson model[7] the case of *critical* damping is usually assumed. For critical damping the ratio is $\gamma/f_{tc}=4\pi$. Although we do not know the precise

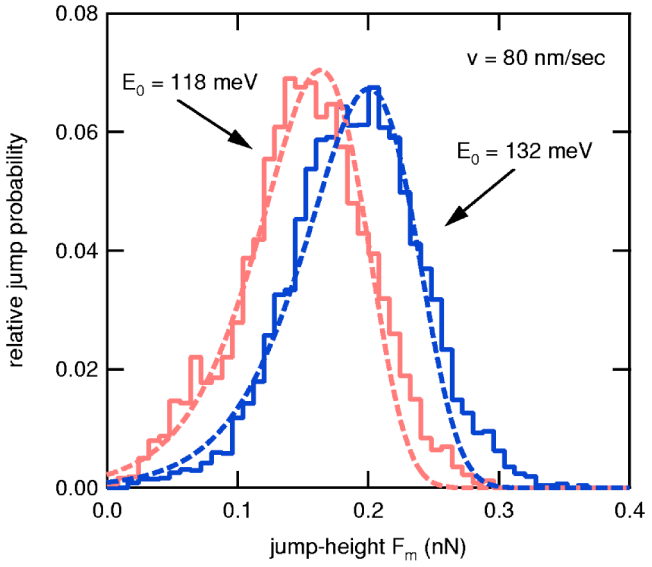

FIG. 9. (Color online) The experimental jump-height distribution functions for a scan speed of 80 nm s^{-1} (solid lines, cityscape shape), which were compiled from the jumps at the side (red) and the center (blue) of the hollow-site rows. The dashed lines are the corresponding best fits with the thermally activated Tomlinson model from Sang *et al.* (Ref. 11) with the energy barrier heights $E_0^{\min}=118$ meV and $E_0^{\max}=132$ meV, respectively.

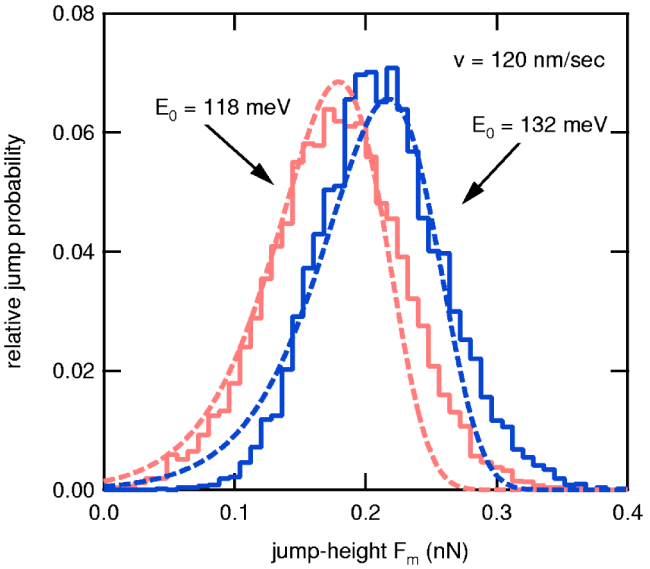

FIG. 10. (Color online) The experimental jump-height distribution functions for a scan speed of 120 nm s^{-1} (solid lines, cityscape shape), which were compiled from the jumps at the side (red) and the center (blue) of the hollow-site rows. The dashed lines are the corresponding best fits with the thermally activated Tomlinson model from Sang *et al.* (Ref. 11) with the energy barrier heights $E_0^{\min}=118$ meV and $E_0^{\max}=132$ meV, respectively.

value of γ in our experiments we will use the value for critical damping, since it represents a defined oscillation behavior. Therefore we use an estimate of $\gamma=9.2\times10^5$ s^{-1}. At this point we note that it would also be possible to obtain the γ coefficient directly from friction measurements above the critical velocity.[18] Alternatively, one could determine the energy barrier height E_0 from the velocity dependence of the friction[10] and extract the friction coefficient γ from the fit to the histogram.

A comparison between experimental and theoretical jump-height distribution functions is shown in Fig. 9 (scan speed of $v=80$ nm s^{-1}). The peak width and the peak position of the experimental curves (solid cityscape lines) are well reproduced by the theoretical curves (broken lines). The peak height and the asymmetry, however, cannot be unambiguously confirmed, which is due to the noise in the experimental histogram. Unfortunately, the noise of the jump-height determination is of comparable magnitude as the statistical noise of the lateral force measurement, and therefore the original distribution function will be superimposed by a Gaussian noise peak. However, the width of the theoretical distribution function is mainly determined by the temperature (and also indirectly by the force calibration), and the reasonable agreement of the experimental and theoretical widths of the distribution function indicates that the spread of the jump-heights is related to the thermally activated Tomlinson model.

The histogram compiled from jumps at the center of the hollow-site rows (solid arrows in Fig. 7) was fitted with a surface barrier potential of $E_0=132$ meV, and the histogram from the jumps at the side of the hollow-site rows (dashed arrows in Fig. 7) was fitted with $E_0=118$ meV. These energy barrier heights are comparable to the values previously found in stick-slip friction experiments.[10,18] In this context it is interesting to note that the absolute value of the fitted barrier heights depends on the friction coefficient γ; however, the difference between the maximum and minimum barrier heights $\Delta E_0=14$ meV is independent of the particular γ value.

A similar good agreement is observed for the diagrams in Fig. 10, which were compiled from jumps at a higher tip base velocity of $v=120$ nm s^{-1}. Best fits were achieved with exactly the same values for γ and E_0, except that the velocity was adjusted to the experimental value, which results in a shift of the curves by 20 pN towards higher force values.

VI. CONCLUSION

In conclusion we have measured atomic scale stick-slip friction on graphite (HOPG). From the friction maps we extract the maximum lateral force, which is necessary to induce a jump. Additionally, we perform a statistical analysis of the jumps. The concept of the jump-height histogram is introduced which directly shows the probability of the tip to jump at a certain lateral bias force. We compare the experimental histograms with the theoretical distribution function from Sang *et al.*[11] which is based on the thermally activated Tomlinson model. We find that the width and the shift of the histograms agree well with the theory, while the expected asymmetry of the histograms cannot be confirmed within the noise of the experiment.

However, the histograms depend strongly on the exact position of the tip with respect to the atomic structure of the surface, which is a direct consequence of the two-dimensionality of the surface potential. In fact, the energy

dissipated during one friction loop varies by a factor of 3, depending on the exact tip position. From the fits to our experimental distribution functions we find a correlation between the site dependence of the friction loops with different energy barriers of the surface potential, ranging from 118 to 132 meV. This means that already a small variation of the effective surface energy barrier by about 10% can have a large effect on the lateral friction. In this context it should be noted that it has been found recently that the friction on HOPG can also vary dramatically depending on the scan angle.[19]

ACKNOWLEDGMENTS

We gratefully acknowledge continuous support and many useful discussions with H. Hölscher (CeNTech, Germany) and U. D. Schwarz (Yale University, USA).

[1] G. A. Tomlinson Philos. Mag. **7**, 905 (1929).
[2] L. Prandtl, Z. Angew. Math. Mech. **8**, 85 (1928).
[3] G. Binnig, C. Quate, and C. Gerber, Phys. Rev. Lett. **56**, 930 (1986).
[4] C. M. Mate, G. M. McClelland, R. Erlandson, and S. Chiang, Phys. Rev. Lett. **59**, 1942 (1987).
[5] J.-A. Ruan and B. Bhushan, J. Appl. Phys. **76**, 8117 (1994).
[6] U. D. Schwarz, O. Zwörner, P. Köster, and R. Wiesendanger, Phys. Rev. B **56**, 6987 (1997).
[7] H. Hölscher, U. D. Schwarz, O. Zwörner, and R. Wiesendanger, Phys. Rev. B **57**, 2477 (1998).
[8] S. Fujisawa, Y. Sugawara, S. Ito, S. Mishima, T. Okada, and S. Morita, Nanotechnology **4**, 138 (1993).
[9] N. Sasaki, K. Kobayashi, and M. Tsukada, Phys. Rev. B **54**, 2138 (1996).
[10] E. Gnecco, R. Bennewitz, T. Gyalog, C. Loppacher, M. Bammerlin, E. Meyer and H.-J. Gntherodt, Phys. Rev. Lett. **84**, 1172 (2000).
[11] Y. Sang, M. Dube, and M. Grant, Phys. Rev. Lett. **87**, 174301 (2001).
[12] Please note that the barrier height E_0 is defined here as the amplitude of the sinusoidal interaction potential, and not as the difference of top and bottom of the potential.
[13] E. Gnecco, R. Bennewitz, T. Gyalog, and E. Meyer, J. Phys.: Condens. Matter **13**, R619 (2001).
[14] J. E. Sader, I. Larson, P. Mulvaney, and L. R. White, Rev. Sci. Instrum. **66**,3789 (1995).
[15] O. Marti, in *Handbook of Micro/Nano Tribology*, edited by B. Bhushan (CRC, Boca Raton, FL, 1990).
[16] P. Bilas, L. Romana, B. Kraus, Y. Bercion, and J. L. Mansot, Rev. Sci. Instrum. **75**, 415 (2004).
[17] N. Sasaki, M. Tsukada, S. Fujisawa, Y. Sugawara, S. Morita, and K. Kobayashi, Phys. Rev. B **57**, 3785 (1998).
[18] E. Riedo, E. Gnecco, R. Bennewitz, E. Meyer, and H. Brune, Phys. Rev. Lett. **91**, 084502 (2003).
[19] M. Dienwiebel, G. S. Verhoeven, N. Pradeep, J. W. M. Frenken, J. A. Heimberg, and H. W. Zandbergen, Phys. Rev. Lett. **92**, 126101 (2004).